

UNIVERSITY OF  
CANTERBURY

*Te Whare Wānanga o Waitaha*  
CHRISTCHURCH NEW ZEALAND

# ENME302 Assignment 2

*Shallow water gravity waves*

John King

## Contents

<b>1</b>	<b>Code verification</b>	<b>2</b>
1.1	Question 1 . . . . .	2
1.2	Question 2 . . . . .	2
1.3	Question 3 . . . . .	3
1.4	Question 4 . . . . .	3
1.5	Question 5 . . . . .	4
1.6	Question 6 . . . . .	5
1.7	Question 7 . . . . .	6
1.8	Question 8 . . . . .	6
1.9	Question 9 . . . . .	7
1.10	Question 10 . . . . .	7
<b>2</b>	<b>Asteroid impacting Lake Taupō</b>	<b>8</b>
2.1	Question 11 . . . . .	8
2.2	Question 12 . . . . .	10
2.3	Question 13 . . . . .	12
2.4	Question 14 . . . . .	12
2.5	Question 15 . . . . .	13
2.6	Question 16 . . . . .	14
2.7	Question 17 . . . . .	14
2.8	Question 18 . . . . .	14

# 1 Code verification

## 1.1 Question 1

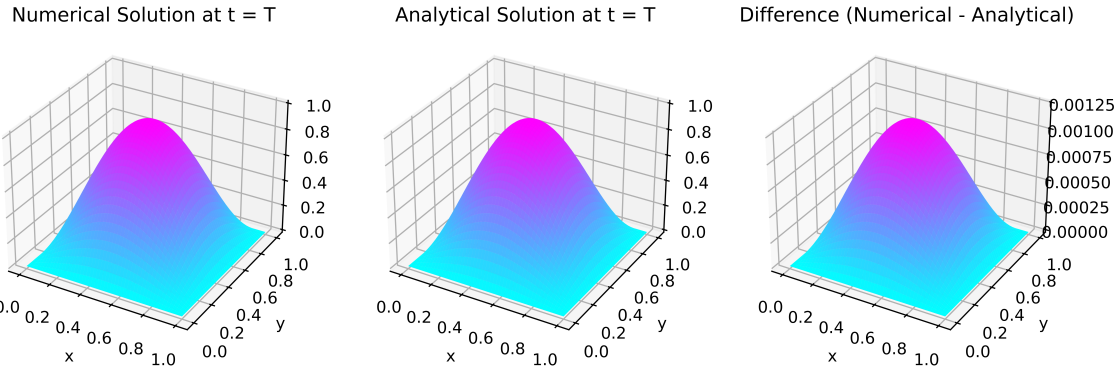


Figure 1: Plots of the numerical and analytical solutions using 3-D surface plots after one oscillation as well as a plot of the difference between the two solutions.

## 1.2 Question 2

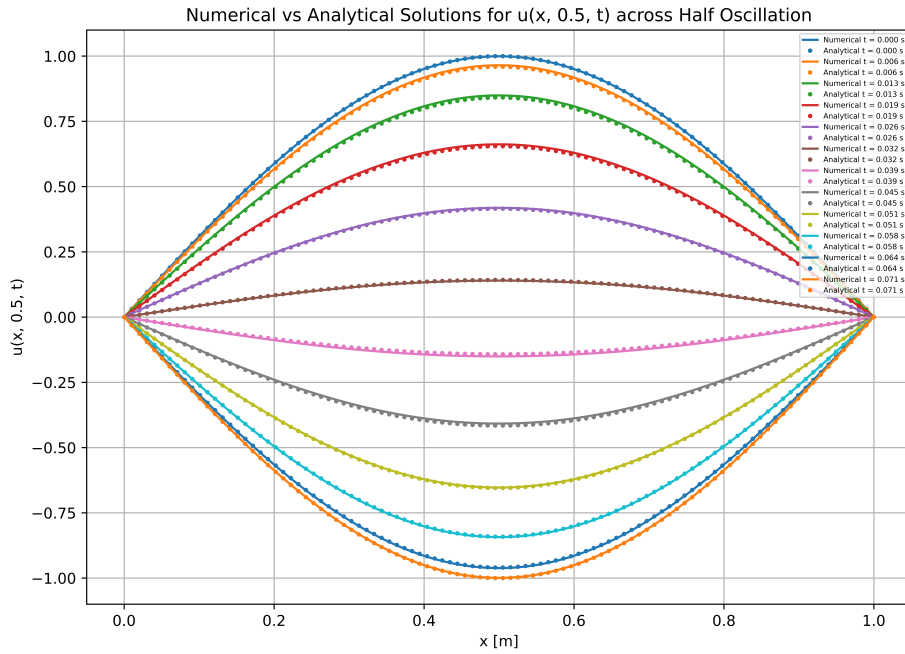


Figure 2: Plots of the line graphs of  $u(x, 0.5 \text{ m}, t)$  against  $x$  for several times across half an oscillation.

### 1.3 Question 3

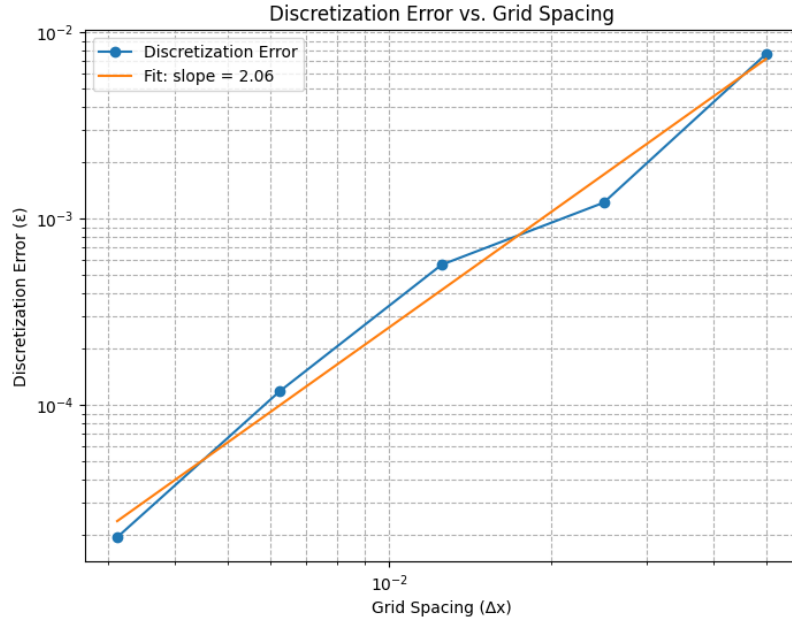


Figure 3: Plot of the discretisation error  $\epsilon$  against grid spacing  $\Delta x$  using a constant Courant number of 0.5 and final time of 1.0 s.

### 1.4 Question 4

#### Comparison Between Numerical and Analytical Solutions

The numerical and analytical solutions using 3-D surface plots after one oscillation are shown in Figure 1. The numerical solution was obtained using the finite difference method with the central difference, explicit scheme, while the analytical solution is derived from the exact expression of the governing equations. The difference plot between the numerical and analytical solutions highlights the regions where the numerical solution diverges from the exact solution. The difference appears to be uniformly distributed across the entire domain, indicating that the numerical method's precision is inherently limited by the chosen scheme.

The line graphs of  $u(x, 0.5 \text{ m}, t)$  versus  $x$  is plotted for several time steps during half an oscillation in Figure 2. These plots compare the numerical and analytical solutions at different points in time, with the numerical solution represented by continuous lines and the analytical solution indicated by markers. By observing these graphs, the evolution of the system across the spatial domain is clearly visualised at each selected time instant. The numerical solution appears to consistently follow the analytical solution closely, indicating accuracy of the numerical method as the system progresses through its oscillatory behavior.

## Convergence Rates

The discretisation error  $\varepsilon$  is plotted against the grid spacing  $\Delta x$  in Figure 3, using a constant Courant number and a fixed final time. This plot shows the linear relationship between the error and the grid resolution. The gradient of the fitted curve shows how the error increases with courser grid spacing at a gradient of 2.06.

The Courant number influences the stability and accuracy of the numerical scheme. A Courant number of 0.5 was chosen for the simulations and by keeping the number constant, stability is ensured across different grid resolutions, and the rate of convergence becomes more evident.

## Verification with method of manufactured solutions

The code was verified using the method of manufactured solutions to ensure that  $g(x, y)$  and  $s(x, y, t)$  were also implemented correctly. The following two manufactured solutions were used:

$$u_{e1} = (x - x^2)(y - y^2) \left( 1 + \frac{1}{2}t \right)$$

$$s = GH(t + 2)(x - x^2 + y - y^2) \quad (4a)$$

$$u_{e2} = (x - x^4)(y - y^4)(1 + t)$$

$$s = 12GH(t + 1) (y^2(x - x^4) + x^2(y - y^4)) \quad (4b)$$

## 1.5 Question 5

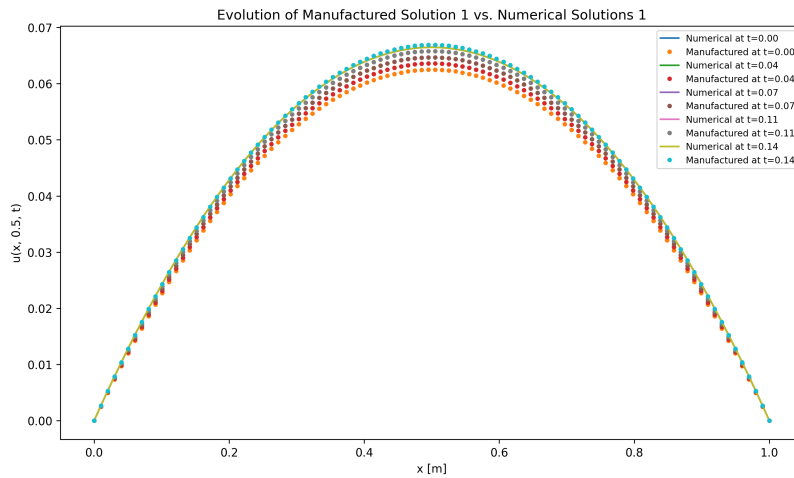


Figure 4: Plot of the evolution of Manufactured solution 1 using line graphs of  $u(x, 0.5 \text{ m}, t)$  against  $x$  for several times.

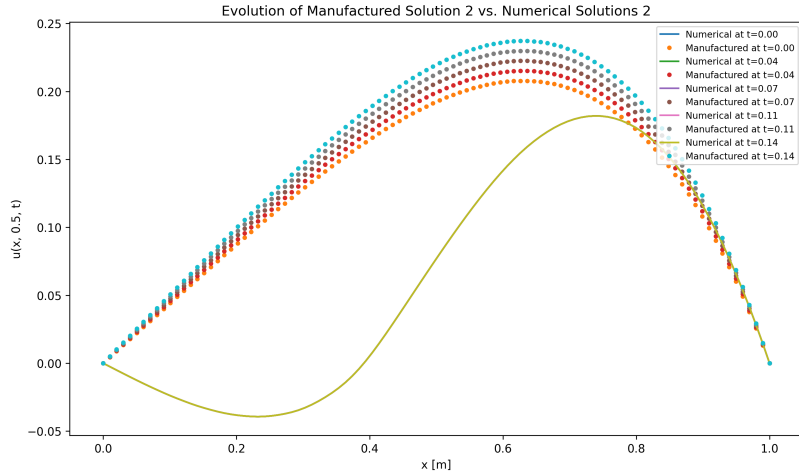


Figure 5: Plot of the evolution of Manufactured solution 2 using line graphs of  $u(x, 0.5 \text{ m}, t)$  against  $x$  for several times.

## 1.6 Question 6

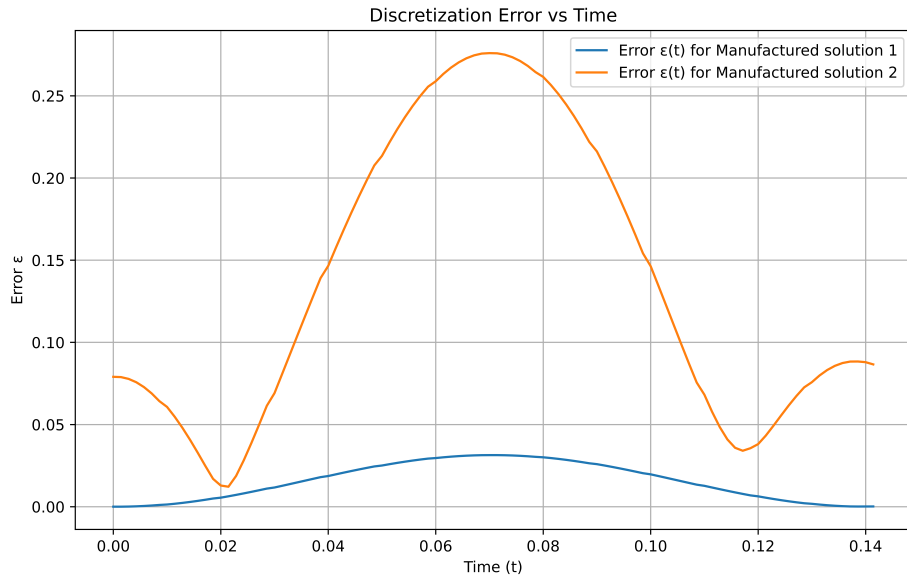


Figure 6: Plot of the error  $\epsilon$  against time  $t$  for each manufactured solution.

## 1.7 Question 7

### Rates of Accumulating Discretisation Error

The discretisation error  $\epsilon$  for both manufactured solutions is plotted against time in Figure 6. The error increases gradually and periodically over time due to the accumulation of numerical artifacts in both cases, as shown in the error versus time plots. However, for finer grids and smaller time steps, the error growth rate is reduced, indicating that the discretisation error can be largely controlled by the spatial and temporal resolutions.

### Physical Sense of Solutions

The manufactured solutions exhibit physically meaningful behaviour, as they are constructed to behave similarly to real-life natural shallow water waveforms. The displacement of the water surface, as shown in Figures 4 and 5, evolves smoothly with each time step for both solutions which is consistent with real-world wave propagation.

### Verification with COMSOL

## 1.8 Question 8

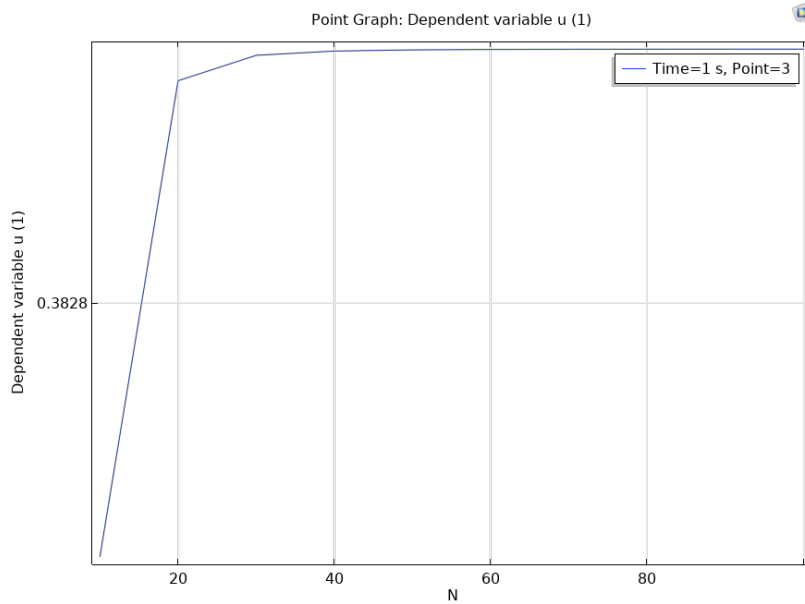


Figure 7: Mesh convergence.

## 1.9 Question 9

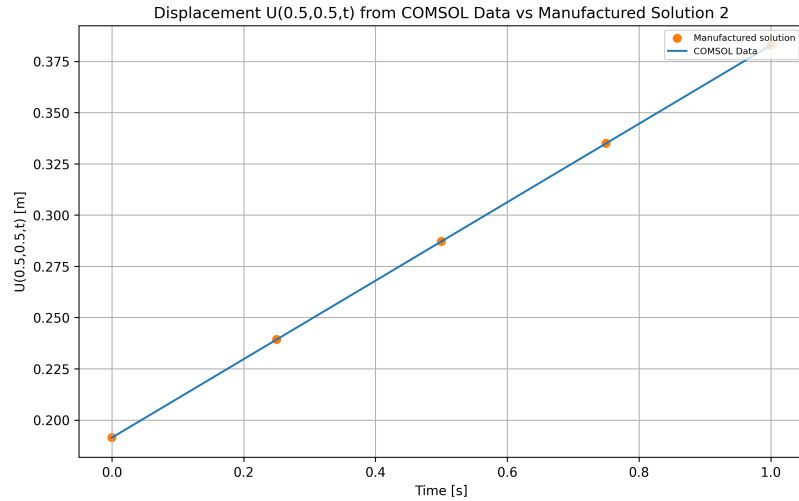


Figure 8: Displacement at  $U(0.5 \text{ m}, 0.5 \text{ m}, t)$  over time, comparing the Manufactured Python Solution 2 with the COMSOL simulation.

## 1.10 Question 10

### Mesh Convergence Analysis

The mesh convergence of the second manufactured solution is shown in Figure 7. The COMSOL simulations display mesh convergence, with the results stabilising as the mesh is refined to 40 or more elements. A too-coarse mesh introduces significant numerical error, while a finer mesh brings the results in line with the Python solution. The results show that while computational complexity increases with finer meshes, a balance is struck where further refining of the mesh yields diminishing returns. For this case, a mesh with 'normal' element sizes was sufficient for convergence and was therefore used.

### Comparison of Results With Python Code

The displacement at  $u(0.5 \text{ m}, 0.5 \text{ m}, t)$  was plotted against time  $t$  using both the Python and COMSOL solutions, as shown in Figure 8. The comparison between the Python code and COMSOL shows similar results for both displacement and error accumulation. The Python solution, despite being a more simplistic model, captures the key wave displacement dynamics effectively when compared with the more sophisticated COMSOL model.

## 2 Asteroid impacting Lake Taupō

Axisymmetric assumption

### 2.1 Question 11

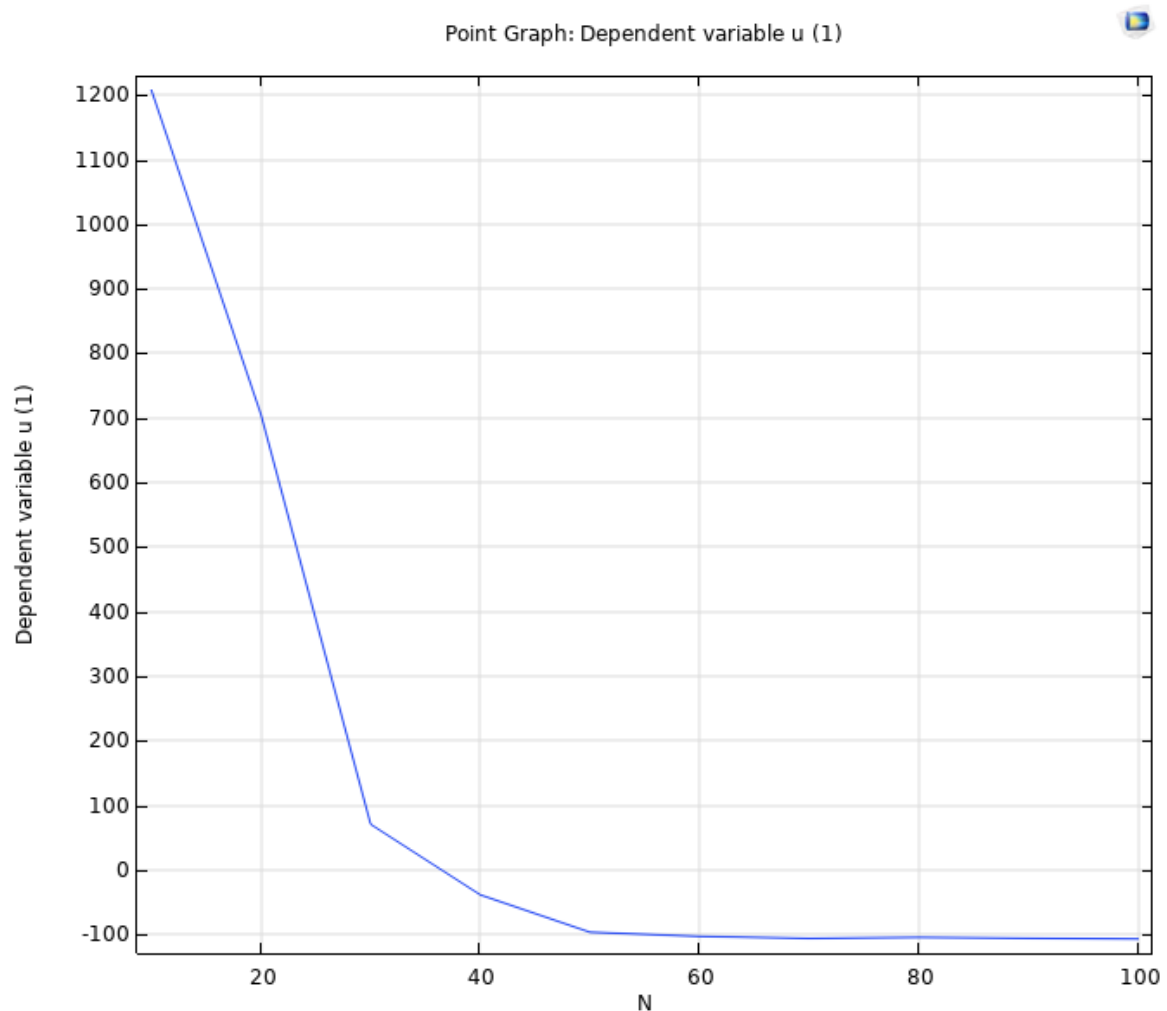


Figure 9: Mesh convergence for axisymmetric 1-D case.

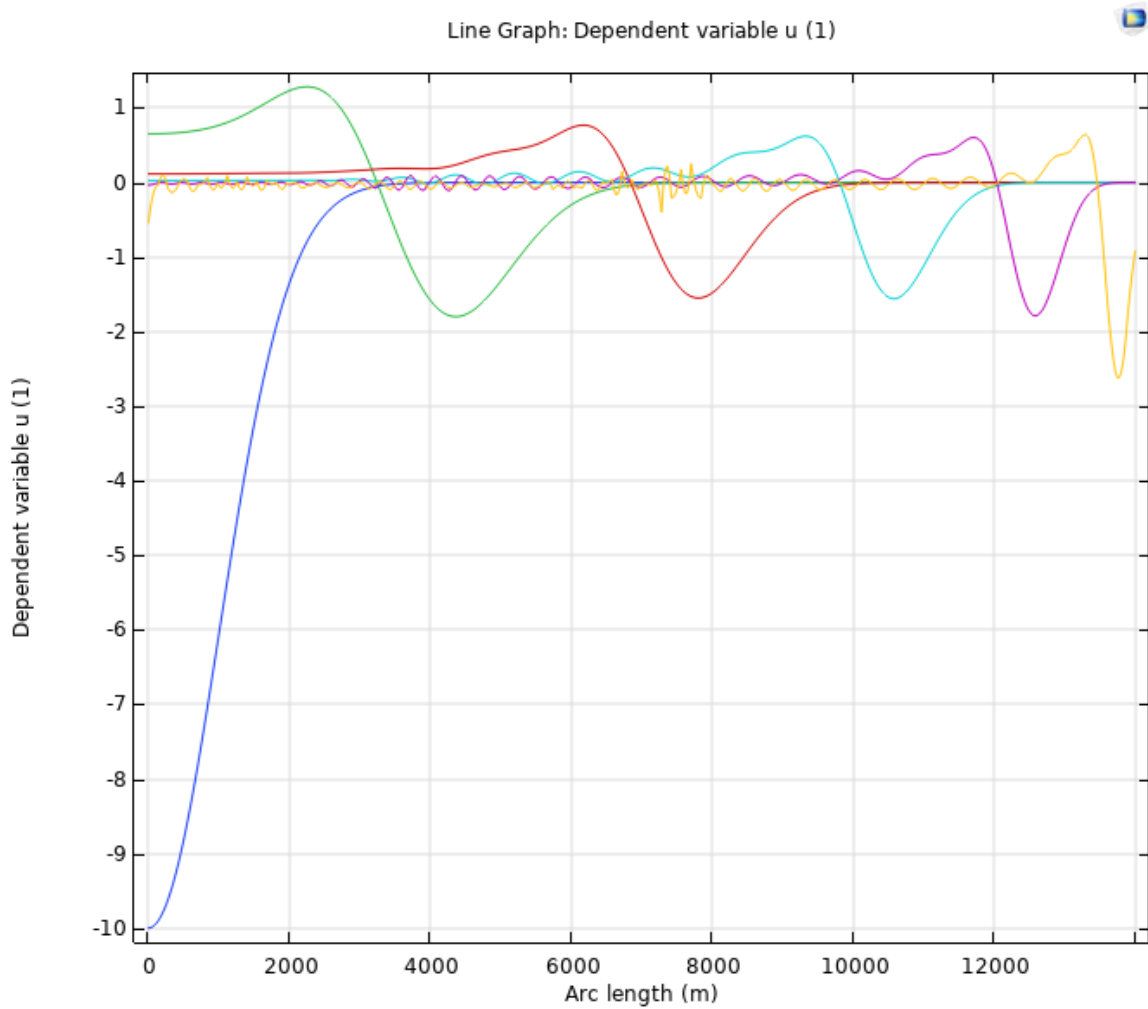


Figure 10: Evolution of the displacement throughout the lake  $u(r, t)$ .

## 2.2 Question 12

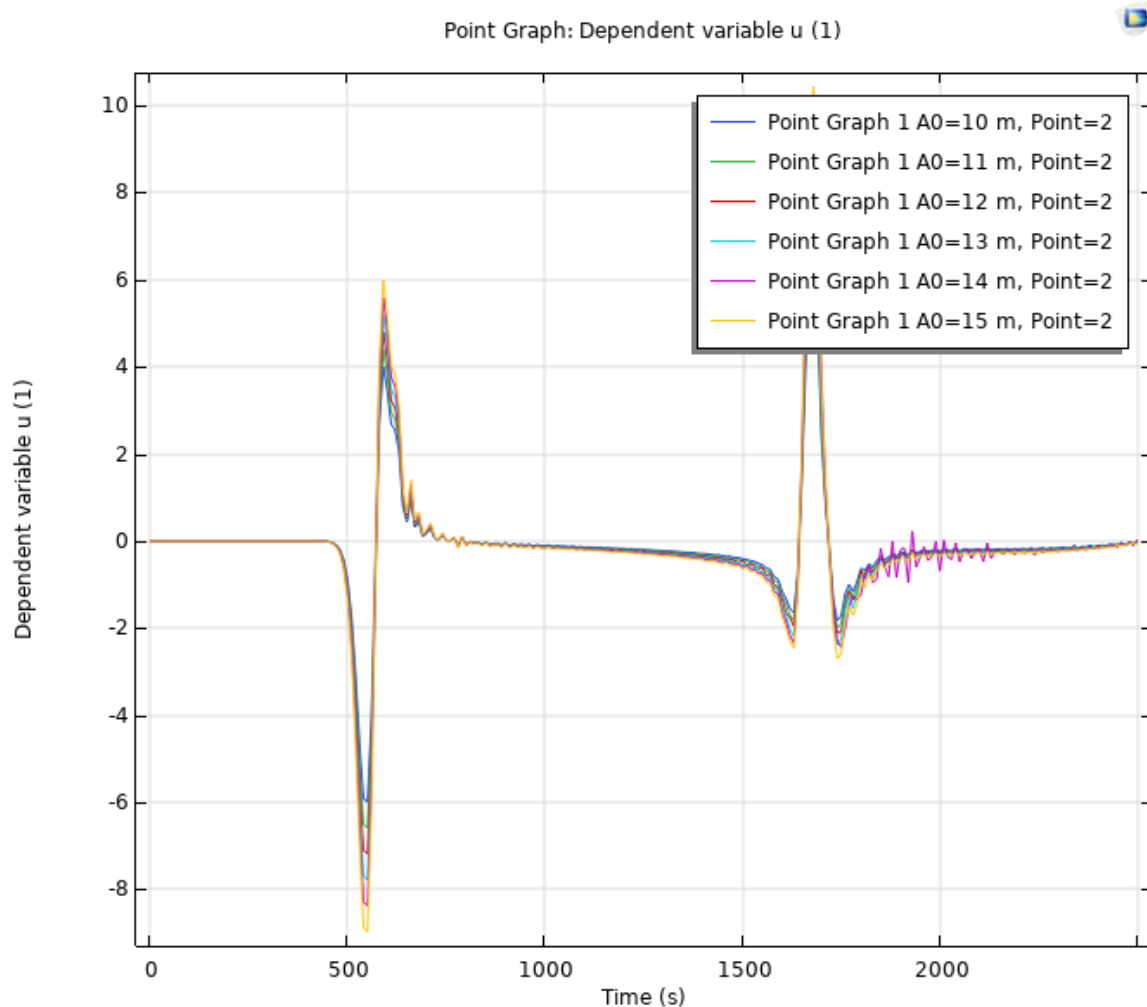


Figure 11: Sensitivity analysis of  $A_0$ .

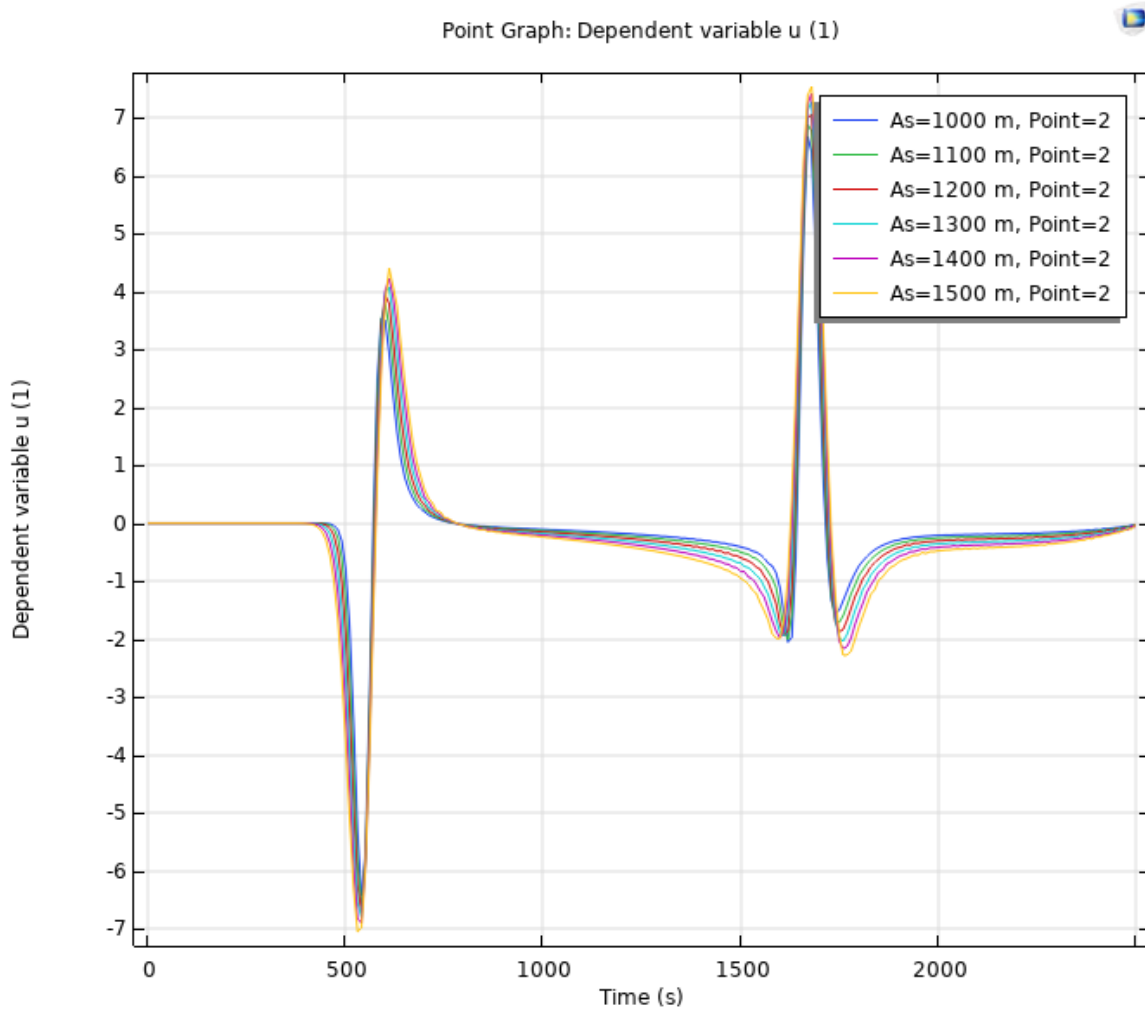


Figure 12: Sensitivity analysis of As.

### 2.3 Question 13

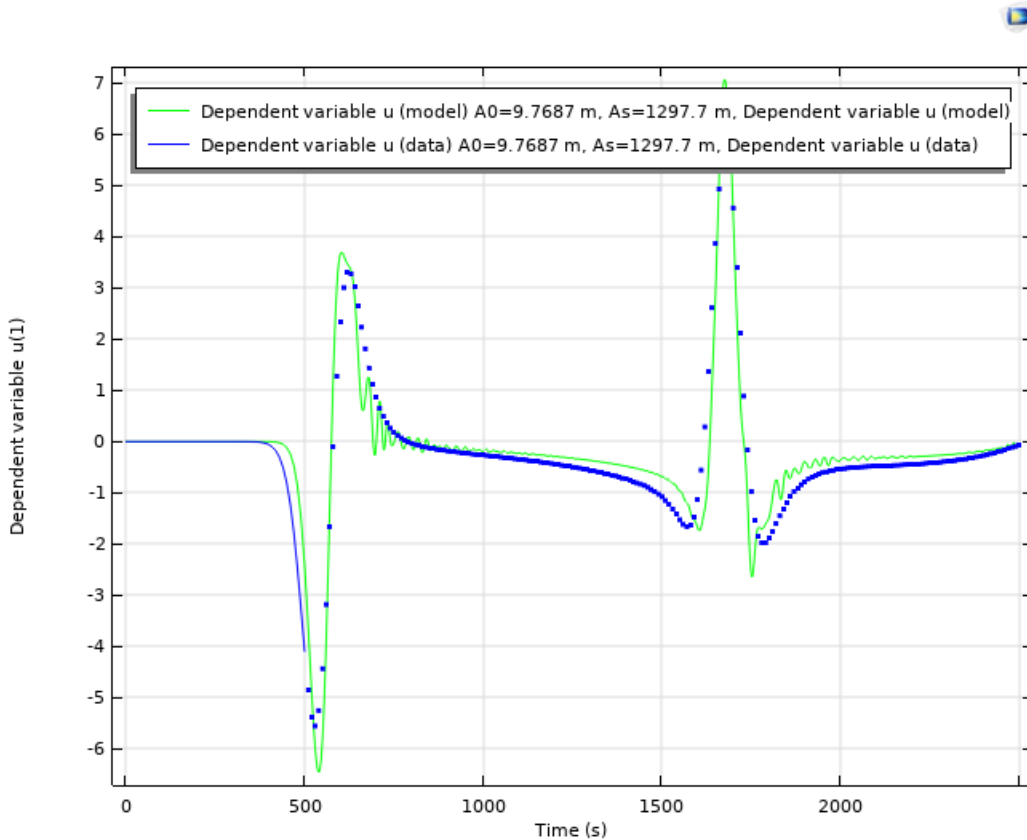


Figure 13: Recovered A0 and As parameters.

### 2.4 Question 14

#### Mesh Convergence

The mesh convergence study shows that sufficient refinement is needed to capture the key wave dynamics, especially near the yacht's location. The COMSOL simulations display mesh convergence, with the results stabilising around -100 as the mesh is refined to 50 or more elements.

#### Hydrograph Sensitivity on A0 and As

The displacement,  $u(r = R, t)$ , was plotted against time with varying A0 and As parameters as shown in Figures 11 and 12. The sensitivity analysis A0 mainly boosts the wave amplitude and As mainly affects the wavelength and spacial spread. The unknown parameters, A0, and As, were recovered using a parameter estimation study on the hydrograph data from hydrograph1D.dat, as

shown in Figure 13. The recovered parameters were  $A_0 = 9.77$  m and  $A_s = 1297.70$  m.

### Maximum Deflections Experienced by the Yacht

The evolution of the displacement throughout the lake over time is shown in Figure 10. The maximum deflections observed are significant but depend heavily on the initial dip parameters  $A_0$  and  $A_s$ . The maximum dip experienced by the yacht using  $A_0 = 10$  m was -10 m.

### Physical Sense of Solutions

The time taken for the waves to reach the yacht aligns with predictions based on the speed of shallow water waves.

### Circular 2-D domain

#### 2.5 Question 15

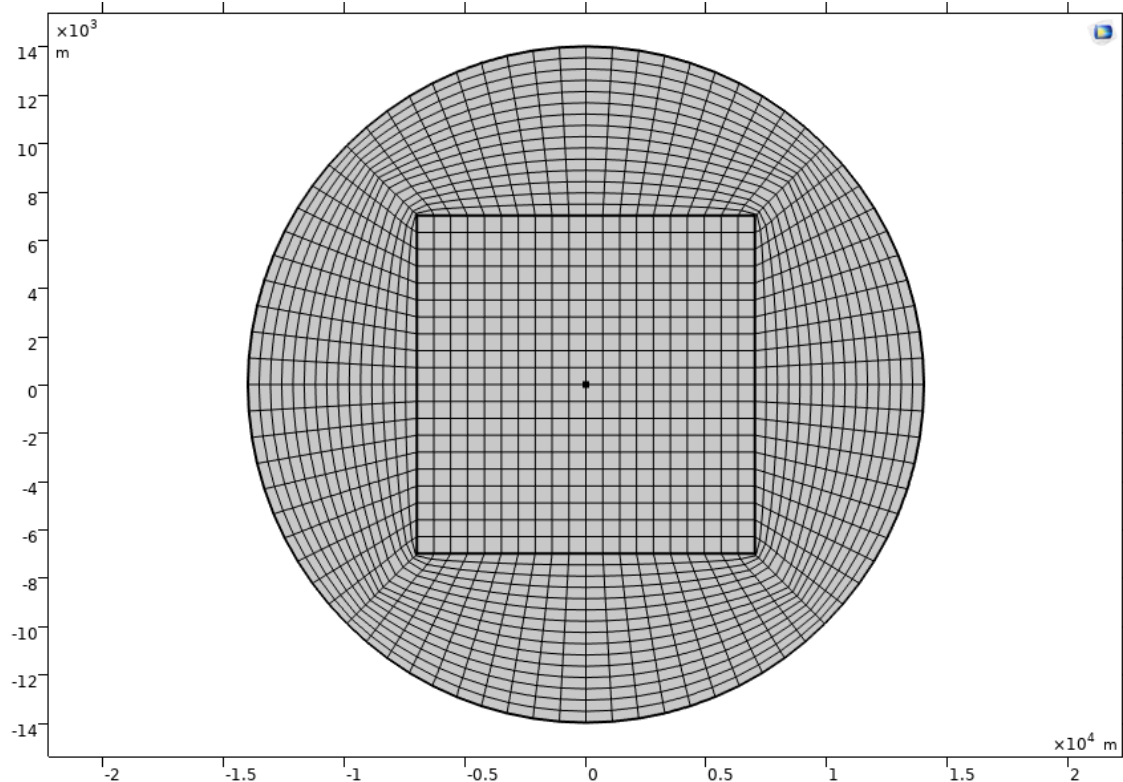


Figure 14: Resulting mesh of a structured OH-grid of the domain.

## 2.6 Question 16

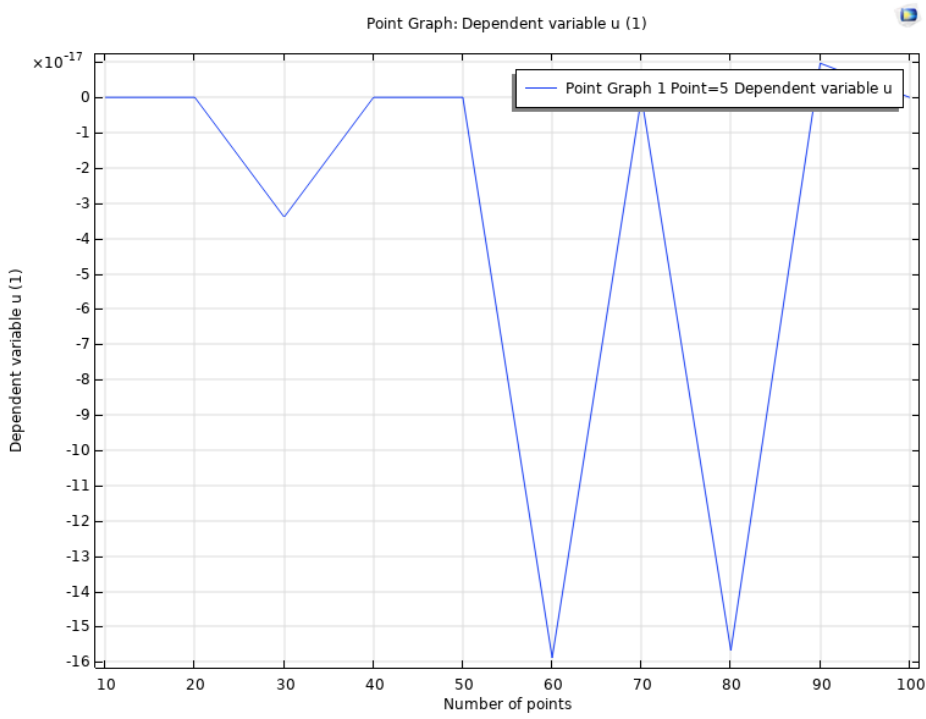


Figure 15: Mesh convergence of a structured OH-grid of the domain.

## 2.7 Question 17

-

## 2.8 Question 18

### Mesh Convergence

The structured OH-grid allows for a smooth transition between mesh sizes, and the mesh convergence study confirms that refinement leads to more accurate results, especially for capturing the wave reflections from the lakefront.

### Critical Review of Modelling Assumptions

The assumptions made throughout the assignment, including homogeneous boundary conditions, a Gaussian initial dip, and the axisymmetric simplification, are mostly valid for an idealized sce-

nario. However, real-world complexities like wind effects, variable sediment composition, and non-homogeneous boundaries could alter the wave dynamics, requiring further refinement in future models.

### **Physical Sense of Solutions**

The final 2-D model captures the wave dynamics in Lake Taupō without the simplifications of axisymmetry. The results show a clear evolution of waves propagating from the impact point and interacting with the lakefront, which matches the expected behavior of real waves in a circular basin.